Frontiers in Bioscience Landmark

Front. Biosci. (Landmark Ed) **2026**; 31(4): 48544
https://doi.org/10.31083/FBL48544

Original Research

Inactivation of NONO by Auranofin or RNA Interference Triggers Lethal Oxidative Stress in Neuroblastoma Cells

Sofya S. Pogodaeva[1,†], Olga O. Miletina[1,†], Lidia V. Mammadova[1], Nadezhda V. Antipova[2], Alexander A. Shtil[3], Oleg A. Kuchur[1,4,*]

[1]Center for Molecular and Biological Technologies, ITMO University, 190002 Saint Petersburg, Russia
[2]Laboratory of Membrane Bioenergetics, Shemyakin-Ovchinnikov Institute of Bioorganic Chemistry, Russian Academy of Sciences, 117997 Moscow, Russia
[3]Laboratory of Tumor Cell Death, Blokhin National Medical Research Center of Oncology, 115522 Moscow, Russia
[4]Laboratory for Bio and Chemoinformatics, School of Computer Science, Physics and Technology, Higher School of Economics, 194100 Saint Petersburg, Russia
*Correspondence: oakuchur@itmo.ru (Oleg A. Kuchur)
[†]These authors contributed equally.

Academic Editors: Natarajan Aravindan and Wei-Lin Jin
Submitted: 25 November 2025 Revised: 12 March 2026 Accepted: 26 March 2026 Published: 22 April 2026

Abstract

Background: Neuroblastoma (NB), a transcriptionally driven pediatric malignancy, exhibits a remarkable clinical and biological heterogeneity. Two major subtypes, adrenergic and mesenchymal, are differentially governed by distinct subsets of transcription factors that constitute the core regulatory circuitry (CRC). The adrenergic subtype is often associated with *MYCN* oncogene amplification and is particularly aggressive and therapy-resistant, underscoring the need for novel therapeutic targets. **Methods**: Gene knockdown with siRNAs, qRT-PCR, flow cytometry-assisted measurements of intracellular oxidation and cell death parameters, immunoblotting, cytotoxicity assays (MTT, colony formation). **Results**: We identified the multifunctional non-POU domain-containing octamer-binding (NONO) protein as a guardian of individual CRC genes, thereby promoting the survival of NB cells with different *MYCN* copy numbers. In the *MYCN*-amplified Kelly cell line, intracellular oxidation induced by auranofin, an inhibitor of thioredoxin reductase 1 (TrxR1), rapidly down-regulated *NONO* mRNA and protein levels. Conversely, *NONO* knockdown by RNA interference (siNONO) also triggered intracellular oxidation. These effects were less pronounced in the SK-N-AS cell line carrying a single MYCN copy, as well as in non-malignant HS5 fibroblasts. In Kelly and IMR-32 cells, siNONO attenuated auranofin-induced activation of CRC genes, namely, heart and neural crest derivatives expressed 2 (*HAND2*) and paired-like homeobox 2B (*PHOX2B*). Furthermore, the Kelly cells were more sensitive to combinations of sublethal auranofin concentrations and siNONO than the counterparts with single *MYCN* copy. Importantly, *MYCN*-amplified cells demonstrated a significantly suppressed clonogenic survival 14 days after transient exposure to these combinations compared with each agent alone; HS5 fibroblasts were largely spared. **Conclusions**: Our findings reveal a new role for the transcriptional regulator NONO in maintenance of the cellular redox balance and justify the strategy of therapeutic targeting of *MYCN*-amplified tumors vulnerable to oxidative stress.

Keywords: auranofin; core regulatory circuitry; MYCN; NONO; neuroblastoma; oxidative stress

1. Introduction

Neuroblastoma (NB) is a pediatric malignancy of the sympathetic nervous system, arising from embryonic neural crest precursors. It shows extreme clinical heterogeneity: some tumors spontaneously regress, whereas others progress relentlessly despite intensive multimodal therapy [1–3]. About half of patients present with high-risk disease, for which 5-year survival remains below 50% [4]. Like most childhood tumors, NB has a low somatic mutation burden; instead, widespread epigenetic and transcriptional deregulation are predominant. A hallmark of high-risk NB is amplification of the *MYCN* oncogene, an established marker of the aggressive disease. Other factors such as activating *ALK* mutations or 11q deletions occur in subsets of cases [5–8]. Thus, NB is better characterized by a 'transcriptional burden' [9], underscoring the importance of gene-regulatory therapeutic programs.

Genome-wide expression profiling has revealed two major NB cell states termed the adrenergic (ADRN) and mesenchymal (MES) subtypes [10,11]. The ADRN subtype is typically linked to *MYCN* gene amplification and is defined by a cohort of transcription factors (PHOX2B, HAND2, GATA3, ISL1, TBX2, ASCL1, *etc.*) that regulate each other at the level of gene expression. These factors form a self-reinforcing core regulatory circuitry (CRC) [12,13]. In contrast, MES cells express a different lineage program, e.g., PRRX1, YAP/TAZ and SNAI1, and resemble neural-crest–derived MES phenotypes. This state tends to be more chemoresistant and invasive, and may expand after treatment pressure [14–16]. Importantly, both states can undergo transition and transdifferentiate in the course

of therapy [17,18]. This transcriptional heterogeneity and plasticity, along with low immunogenicity, complicates the treatment.

Current regimens for high-risk NB include intensive chemotherapy, radiotherapy, anti-GD2 immunotherapy and autologous stem-cell rescue [19–21]. However, the majority of tumors relapse. Over half of children with high-risk NB eventually experience disease recurrence, which significantly reduces survival rates [22,23]. Conventional therapies do not specifically address the individual molecular 'portraits' of NB subtypes; therefore, the tumors can escape standard cytotoxic agents [24–26]. These limitations highlight the need for novel approaches that target the biological peculiarities of NB.

CRC targeting has emerged as an attractive strategy. The genome-wide screens showed that MYCN, HAND2, ISL1, PHOX2B, GATA3 and TBX2 transcription factors are essential for *MYCN*-amplified NB [27,28]. Disruption of this circuitry profoundly impairs NB growth. Combined inhibition of transcriptional proteins BRD4 and CDK7 caused rapid loss of CRC transcription and synergistically suppressed *MYCN*-amplified tumors [29]. These reports as well as other studies emphasized a network of distinct CRC members and auxiliary survival pathways that act in concert to promote NB cell survival [30].

Among transcriptional mechanisms in NB, the non-POU domain-containing octamer-binding protein (NONO or p54nrb) deserves a special heed. NONO, a multifunctional DNA/RNA-binding protein, has been recently identified as a master regulator of oncogenic transcription in NB [31,32]. NONO binds to 5′-ends of introns and to long non-coding RNAs (lncRNAs) including *MYCN* transcript, promoting the expression of oncogenes [33]. Through these interactions, NONO 'guards' CRC and amplifies *MYCN* signaling. Clinically, high *NONO* expression correlates with aggressive NB and poor prognosis [34].

Thus, NONO is an important regulator of neuroblastoma conditions, and its pharmacological inhibition is preferred as it appears to be a promising strategy for the NB treatment. However, NONO has long been considered undruggable since this protein lacks an enzymatic structure; only very recently the small molecular weight compound that disrupts NONO-RNA interaction has been introduced [35–37]. Nevertheless, evidence has been reported in favor of NONO inhibition as a result of metabolic deregulation.

Auranofin is a clinically approved irreversible inhibitor of the antioxidant enzyme thioredoxin reductase 1 (TrxR1) [38]. Consequently, auranofin forces intracellular accumulation of reactive oxygen species (ROS). This effect has been used for induction of oxidative stress in neurogenic tumors [39–41]. Notably, *MYCN*-amplified NB cells rely on robust redox buffers; therefore, these cells may be particularly vulnerable to the shift of redox balance to oxidation [42]. Intriguingly, Hou *et al.* [43] have shown that auranofin can inactivate NONO in glioblastoma. Although the mechanism of inhibition remained to be elucidated, this pivotal observation set the stage for a detailed investigation of the role of NONO in specific metabolic responses as well as for therapeutic combinations to enhance intracellular oxidation in NB cells.

In this study, we investigated whether intracellular oxidation is mechanistically linked to NONO inactivation, deregulation of individual CRC genes and death of NB cells carrying different numbers of *MYCN* copies. The CRC genes *PHOX2B* and *HAND2* were chosen because the former transcription factor reflects the integrity of ADRN lineage-determining program whereas *HAND2* participates in enhancer-dependent transactivation and *MYCN*-mediated proliferation [28,44].

2. Materials and Methods

2.1 Chemicals

Reagents were purchased from Dia-M, Moscow, Russia unless specified otherwise.

2.2 Cell Culture

The human NB cell lines with (Kelly and IMR-32) or without (SK-N-AS, SK-N-SH, SH-SY5Y) *MYCN* amplification were used. All cell lines were purchased from the American Type Culture Collection (Manassas, VA, USA). The HCT116 (colorectal adenocarcinoma; collection of the Institute of Cytology, Russian Academy of Sciences, Saint-Petersburg, Russia) and A549 (lung adenocarcinoma; Biolot, Moscow, Russia) cell lines were used as transformed non-neuronal control. The bone marrow-derived HS5 fibroblast cell line (gift of Dr. T. Lebedev, Engelhardt Institute of Molecular Biology, Russian Academy of Sciences, Moscow, Russia) was a non-malignant counterpart. The Kelly and HS5 cell lines were propagated in RPMI-1640 with 10% fetal bovine serum (Biolot, Moscow, Russia) and 100 µg/mL gentamicin. The IMR-32, SK-N-SH and SH-SY5Y cells were grown in Eagle's Minimum Essential Medium supplemented with 10% serum and 100 µg/mL gentamicin. The HCT116 and A549 cells were grown in Dulbecco's Modified Eagle Medium with 10% serum and 100 µg/mL gentamicin. The SK-N-AS cells were cultured in the same medium with high glucose and 1% non-essential amino acids. Cells were propagated at 37 °C, 5% CO_2 in a humidified atmosphere. All cell lines were validated by STR profiling and found negative for *Mycoplasma* (MycoReport kit, Evrogen, Moscow, Russia).

2.3 Compounds and Cell Treatment

Auranofin (Astellas Pharma, Tokyo, Japan) was dissolved in 10 mM dimethyl sulfoxide and stored at 20 °C prior to the experiments. For transient gene knockdown, five small interfering RNAs (siRNAs) were used: *NONO*, *MYCN*, *HAND2*, *PHOX2B* (CRC gene-specific) and siRNA to *GFP* (unrelated control). All siRNAs (DNA Synthesis, Moscow, Russia; Table 1) were transfected with GenJect

liposomes 40 (Molecta, Moscow, Russia): 2 µL siRNA, 125 nM liposomes in 35 mm Petri dish for 24 h according to the manufacturer's instructions. Gene knockdown was registered 24 h post transfection. Two to three variants of each siRNA sequence were tested to achieve the most pronounced and reproducible knockdown. In combination experiments, cells were transfected with the respective siRNAs; 24 h later fresh medium supplemented with auranofin was added, and cells were incubated for 14 days followed by cytotoxicity assays (see below).

Table 1. Sequences of siRNAs.

Target gene	siRNA	Sequence
MYCN	Sense	5′-GCUUUUGCUGGAAAAGGAAAAdTdT
	Antisense	dTdTUUCCUUUUCCAGCAAAAGCUG-5′
NONO	Sense	5′-GCGACAGCAGGAAGGAUUCAAdTdT
	Antisense	dTdTCGCUGUCGUCCUUCCUAAGUU-5′
HAND2	Sense	5′-GUGUAAACGUUGUAAGUAUUCdTdT
	Antisense	dTdTAUACUUACAACGUUUACACCU-5′
PHOX2B	Sense	5′-UAUGUUCACAAACAUAGUCCAdTdT
	Antisense	dTdTGACUAUGUUUGUGAACAUAAU-5′
GFP	Sense	5′-GAACGGCAUCAAGGUGAACdTdT
	Antisense	dTdTCUUGCCGUAGUUCCACUUG-5′

siRNA, small interfering RNA; NONO, non-POU domain-containing octamer-binding; HAND2, heart and neural crest derivatives expressed 2; PHOX2B, paired-like homeobox 2B; GFP, green fluorescent protein.

2.4 Intracellular Detection of Reactive Oxygen Species

After incubation with auranofin without or with siRNAs, cells were loaded with 5 µM 2′,7′- dichlorodihydrofluorescein diacetate ($DCFH_2$-DA), incubated for 60 min at 37 °C, then washed with phosphate buffered saline pH7.4 (PBS), harvested by centrifugation (500 g, 5 min) and resuspended in 200 µL PBS. Fluorescence intensity was analyzed on a CytoFlex B2-R2-V0 flow cytometer (Beckman Coulter, Brea, CA, USA) (excitation/emission settings 493/523 nm; FITC channel, 488 nm laser). Hydrogen peroxide (0.5 mM) was used as a control for induction of intracellular oxidation.

2.5 Total RNA Extraction and qRT-PCR Analysis

Isolation of total RNA from cells was performed with the ExtractRNA buffer (Evrogen, Moscow, Russia) according to the manufacturer's protocol. cDNA was synthesized from 2 µg total RNA preparation using MMLV reverse transcriptase: 25 °C 10 min, 42 °C 50 min, 70 °C 10 min, 10 °C 10 sec. The PCR mixture contained 1 µg cDNA, 5x qPCR SYBR Green I, forward and reverse primers (10 µM each; Table 2), and nuclease-free H_2O.

Amplification conditions:

- Stage 1 (1 cycle): 94 °C 3 min, 60 °C 40 sec, 72 °C 40 sec;
- Stage 2 (28–30 cycles): 94 °C 10 sec, 60 °C 10 sec, 72 °C 20 sec;
- Stage 3 (1 cycle): 72 °C 3 min;
- Stage 4 (storage): 4 °C.

After the completion of reactions, the relative expression was determined by the ΔCt method, where Ct (threshold cycle) is the cycle at which the fluorescence level reaches a certain value (preselected threshold), and Δ is the change in the expression of the gene of interest relative to the transcript selected for normalization (hypoxanthine-guanine phosphoribosyltransferase 1 (*HPRT1*) and *18S RNA* genes; difference ≤2 cycle).

Table 2. Primers for qRT-PCR.

Gene	Primer	Sequence
MYCN	Forward	5′-GAGGACACCCTGAGCGATTC-3′
	Reverse	5′-TTGGTGTTGGAGGAGGAACG-3′
NONO	Forward	5′-ATATGCCACTCCGTGCAAAG-3′
	Reverse	5′-GAAGGAGCCTTCACTGCATC-3′
HAND2	Forward	5′-CTCCAAAATCAAGACCCTGCG-3′
	Reverse	5′-GGCCTTTGGTTTTCTTGTCGT-3′
PHOX2B	Forward	5′-ATTCCTCTGCCTACGAGTCCT-3′
	Reverse	5′-TTTGTAAGGAACTGCGGCG-3′
TXNRD1	Forward	5′-GAGAAAGCTGTGGAGAAGTTTG-3′
	Reverse	5′-CCACAACACGTTCATTGTCTTT-3′
CDKN1A	Forward	5′-AGTCAGTTCCTTGTGGAGC-3′
	Reverse	5′-CATTAGCGCATCACAGTCGC-3′
18S	Forward	5′-AAGTGACGCAGCCCTCTATG-3′
	Reverse	5′-TGGACAACAAGCTCCGTGAA-3′
HPRT1	Forward	5′-TATATCCAACACTTCGTGGGGTC-3′
	Reverse	5′-ACAGGACTGAACGTCTTGCTC-3′

RT-PCR, Reverse Transcription-Polymerase Chain Reaction; *TXNRD1*, thioredoxin reductase 1; *CDKN1A*, cyclin-dependent kinase inhibitor 1A; 18S, 18S ribosomal RNA; *HPRT1*, hypoxanthine-guanine phosphoribosyltransferase 1.

2.6 Immunoblotting

After the completion of treatments, cells were lysed in a buffer containing 50 mM Tris-HCl pH 8.0, 150 mM NaCl, 1% NP-40, 0.1% sodium dodecyl sulfate, 200 µM phenylmethylsulfonyl fluoride, protein inhibitor cocktail (leupeptin, aprotinin and pepstatin, 1 µg/mL each) (Sigma-Aldrich, Burlington, MA, USA). Protein concentration was measured by Bradford assay. Lysates (35 µg total protein per lane) were separated by electrophoresis in 10% sodium dodecyl sulfate-polyacrylamide gels and transferred onto a nitrocellulose membrane (BioRad, Hercules, CA, USA) at 250 mA, 1 h at 4 °C. Membranes were blocked with 5% bovine serum albumin for 30 min at room temperature and incubated with primary antibodies (1:1000) overnight at 4 °C. After washing with Tris-buffered saline-Tween-20,

membranes were incubated with horseradish peroxidase-conjugated secondary antibodies (1:1000, Cell Signaling Tech., Danvers, MA, USA) for 1 h. Signals were detected with Enhanced Chemilumiscence reagent (Thermo Fisher, Waltham, MA, USA) and captured using a gel documentation system ChemiDoc™ Touch (BioRad) with multiple exposure times to ensure linear range of detection. Primary antibodies were: NONO (PAJ818Hu01, Cloud-Clone Corp., Houston, TX, USA), HAND2 (E-AB-61488, Elabscience, Wuhan, Hubei Province, China), MYCN, PHOX2B, β-actin (AF5204, DF9730, AF7018; Affinity Biosci., Changzhou, Jiangsu, China), cleaved PARP-1 (9541S, Cell Signaling Tech.).

2.7 Cytotoxicity Assays

Five thousand cells/well were plated into 96-well plates and left overnight. Auranofin was tested at concentrations 0.1–50 µM. Cells were treated for 72 h at 37 °C, 5% CO_2. Cell viability was determined by 3-(4,5-dimethylthiazol-2-yl)-2,5-diphenyltetrazolium bromide assays (MTT; Sigma-Aldrich, Burlington, MA, USA). Absorbance was registered on a Tecan spectrophotometer (Tecan Spark™, Männedorf, Switzerland) at 570 nm. The percentages of viable cells were calculated as a ratio (OD_{570} in wells with respective auranofin concentrations) to (OD_{570} of vehicle-treated cells) $\times$ 100%.

For colony formation assays, cells were transfected with the respective siRNAs (indicated in Results) for 24 h, then treated with 0.25 µM auranofin for 24 h, plated into 60 mm Petri dishes (100 cells/well, 10 mL of culture media) and incubated at 37 °C, 5% CO_2 for 14 days. Colonies were fixed in methanol, stained with 0.05% crystal violet for 30 min and counted.

For cell cycle analysis, cells were treated as indicated in Results, then detached and collected by centrifugation. Pellets were washed twice with PBS, fixed with 70% ethanol in PBS at –20 °C for 30 min, treated with 25 µg/mL RNase A (Biolot), stained with 20 µg/mL propidium iodide (PI; Fisher Sci., Waltham, MA, USA) for 15–30 min, resuspended in PBS and analyzed on a CytoFlex B2-R2-V0 flow cytometer (Beckman Coulter, Brea, CA, USA) at excitation/emission settings 544/570 nm (TRITC channel, 532 nm laser). Twenty thousand fluorescence events were collected per each sample.

2.8 Characterization of Cell Death

To determine the mode of death, cells were transfected with siRNAs or treated with auranofin as indicated in Results. After the completion of treatments cells were detached from the plastic, pelleted for 1 min at 500 $\times$g, resuspended in warm culture medium and stained with 10 µM oxazolium yellow (YO-PRO™-1; Fisher Sci., Waltham, MA, USA) for 30 min followed by counterstaining with 10 µg/mL PI for 5–10 min. Fluorescence was recorded on a CytoFlex B2-R2-V0 flow cytometer (Beckman Coulter, Brea, CA, USA) in the FITC and TRITC channels, respectively. Twenty thousand fluorescence events were collected per each sample.

2.9 Statistical Analysis

The GraphPad Prism 8.0 program (GraphPad Software, Boston, MA, USA) was used to plot graphs. Results were processed using a one-way ANOVA test. Differences were statistically significant at $*p \leq 0.05$, $**p \leq 0.01$. At least three biological replicates were tested in each experiment.

3. Results

3.1 Auranofin is Preferentially Cytotoxic for Adrenergic Neuroblastoma Cell Lines

The role of NONO in the development of transcriptional deregulation is crucial due to its ability to bind to lncRNAs and promote transcription of oncogenes [33]. Additionally, high NONO expression correlates with NB aggressiveness [34]. Therefore, targeting NONO emerges as a promising strategy for neuroblastoma treatment. Auranofin, an inhibitor of TrxR1, has been implicated in inactivation of NONO protein in neural cells [42,45]. Firstly, we analyzed the cytotoxic effect of auranofin (72 h exposure) on a panel of cell lines. Fig. 1A shows that auranofin was preferentially cytotoxic against *MYCN*-amplified NB cell lines Kelly (~0.39 µM) and IMR-32 (~0.86 µM) and non-*MYCN*-amplified cell lines SH-SY5Y (~0.41 µM) and SK-N-SH (~0.94 µM) cell lines. The SK-N-AS cells (single *MYCN* copy) were less sensitive to auranofin (IC_{50} ~1.39 µM). The HS5 fibroblasts exhibited similar sensitivity as SK-N-AS cells (IC_{50} ~1.87 µM). The least responsive were A549 and HCT116 cells (IC_{50} ~3.54 µM and ~6.95 µM, respectively). Therefore, epithelial cells have less potential of being affected by auranofin compared to MES and neuronal cells.

Differential sensitivity of NB cells was further demonstrated by the cell cycle distribution flow cytometry analysis (Fig. 1B and **Supplementary Fig. 1**). Auranofin elevated the percentage of apoptotic $subG_1$ events in a dose- and time-dependent manner. By 24 h this effect was the strongest in *MYCN*-amplified Kelly cells: cell populations contained ~30–40% and 50–60% apoptotic cells after treatment with 1 µM and 2 µM auranofin, respectively. In IMR-32 cells, $subG_1$ portions were less pronounced. In SK-N-AS and HS5 cells, the respective percentages were only 10–20%. These results confirmed a preferred sensitivity of *MYCN*-amplified NB cells to auranofin compared to non-*MYCN*-amplified NB cell lines.

Next, we evaluated the abundance of *TXNRD1* and *NONO* mRNAs in NB cell lines with different *MYCN* status and in bone marrow fibroblast cell line HS5 after incubation with 0.5 µM auranofin (Fig. 1C). The steady-state levels of *TXNRD1* and *NONO* mRNAs in HS5 cells were insignificantly affected by auranofin by 2–6 h. This can be

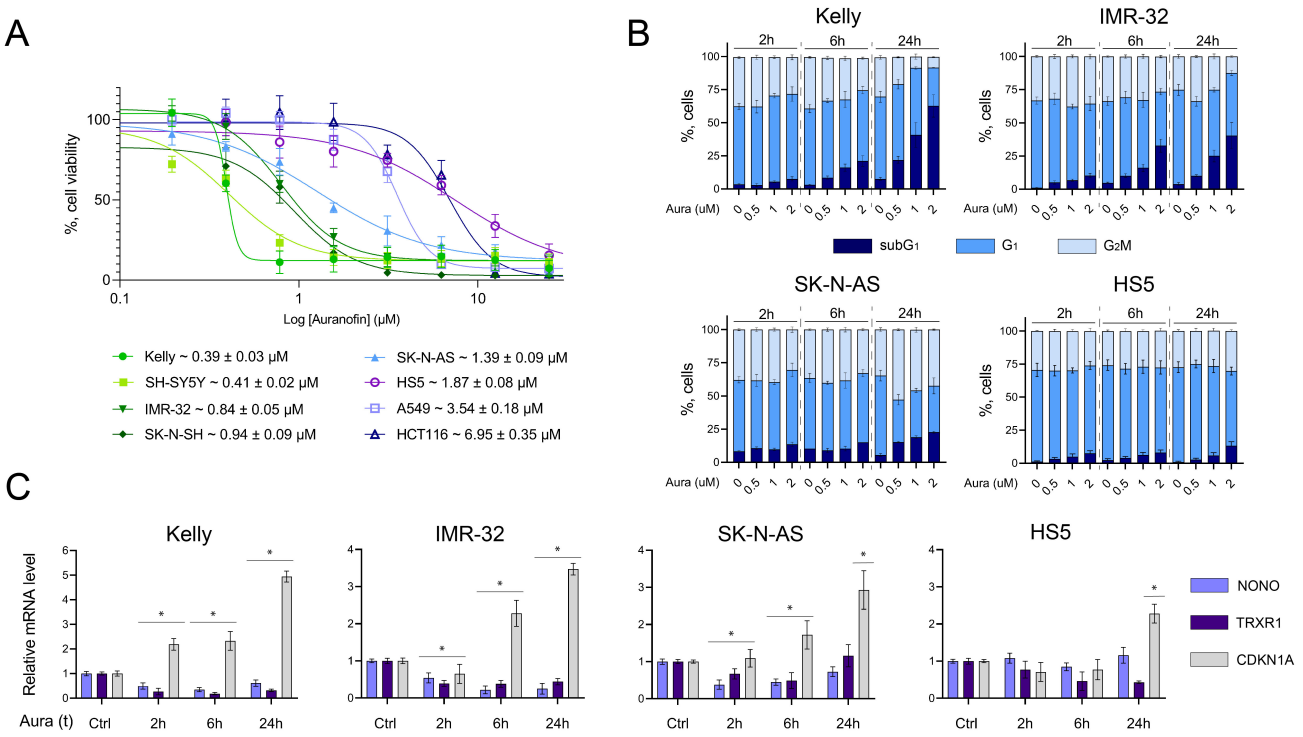

Fig. 1. The effects of auranofin on cell viability, cell cycle distribution and gene expression. (A) Dose response of the cell lines panel to auranofin (72 h, MTT assay). (B) Cell cycle distribution in auranofin-treated cells. Results are shown as mean ± standard errors, n = 3, 20,000 events per sample. (C) Time course of steady-state levels of *NONO, TXNRD1* and *CDKN1A* (normalized to *HPRT1* signal) in response to 0.5 μM auranofin. Levels of each transcript in untreated cells were taken as 1.0 (control). Data are presented as mean ± standard errors (n = 3). Bars above the column groups show statistical significance relative to the control. *$p \leq 0.05$. Aura, auranofin; (t), time, h.

associated with the activity of antioxidant systems potent in HS5 cells [46,47]. In NB cell lines, the level of *TXNRD1* and *NONO* mRNAs significantly decreased as early as by 2 h with auranofin. The strongest effect was observed in *MYCN*-amplified Kelly and IMR-32 cell lines, further substantiating their preferential sensitivity to auranofin-mediated NONO downregulation. In the SK-N-AS cells at 2–6 h the abundance of *TXNRD1* and *NONO* mRNAs decreased significantly, whereas by 24 h these values returned to control. In contrast, the steady-state levels of *CDKN1A* mRNA increased ~3–4-fold, arguing against general down-regulation of transcription in auranofin-treated cells.

3.2 Individual CRC Genes are Differentially Regulated by Auranofin and siNONO

Next, we investigated whether auranofin differentially regulates individual CRC genes across three NB cell lines compared to non-malignant counterparts. As shown in Fig. 2A, treatment with gene-specific siRNAs was efficient: siMYCN attenuated *MYCN* mRNA ~2–3-fold; a similar extent of *NONO* down-regulation was achieved with siNONO. Importantly, auranofin and *MYCN*/*NONO* siRNAs differentially influenced the expression of *HAND2* and *PHOX2B* genes. In Kelly and IMR-32 cells, auranofin activated these genes ~2-fold, and this activation was prevented by siNONO but not by siMYCN. In SK-N-AS and HS5 cells, auranofin evoked minor effects (<1.5-fold) on *HAND2* and *PHOX2B* mRNAs; again, siNONO attenuated the steady-state levels of these transcripts (Fig. 2A). Results of RT-PCR experiments were replicated at the protein level (Fig. 2B). Furthermore, siRNAs alone and in combination with auranofin caused PARP-1 cleavage in Kelly and SK-N-AS cell lines. Neither siMYCN nor siNONO alone triggered PARP-1 cleavage in HS5 fibroblasts. Only the combination of siNONO and auranofin was apoptotic. These results confirmed that HS5 fibroblasts were less sensitive to siNONO- and auranofin-induced apoptosis compared to Kelly and SK-N-AS NB cells.

The analysis of cell cycle distribution showed that the *MYCN*-amplified Kelly cell line was sensitive to siRNA-mediated *NONO* suppression: the portion of nuclei with fragmented DNA ($subG_1$ events) increased up to 60%, in contrast to cell lines carrying a single *MYCN* copy (Fig. 2C and **Supplementary Fig. 2**). Thus, auranofin and *NONO* knockdown synergized in the decrease of the factors relevant to NB cell survival. These results led us to test the therapeutic meaningfulness of these combinations.

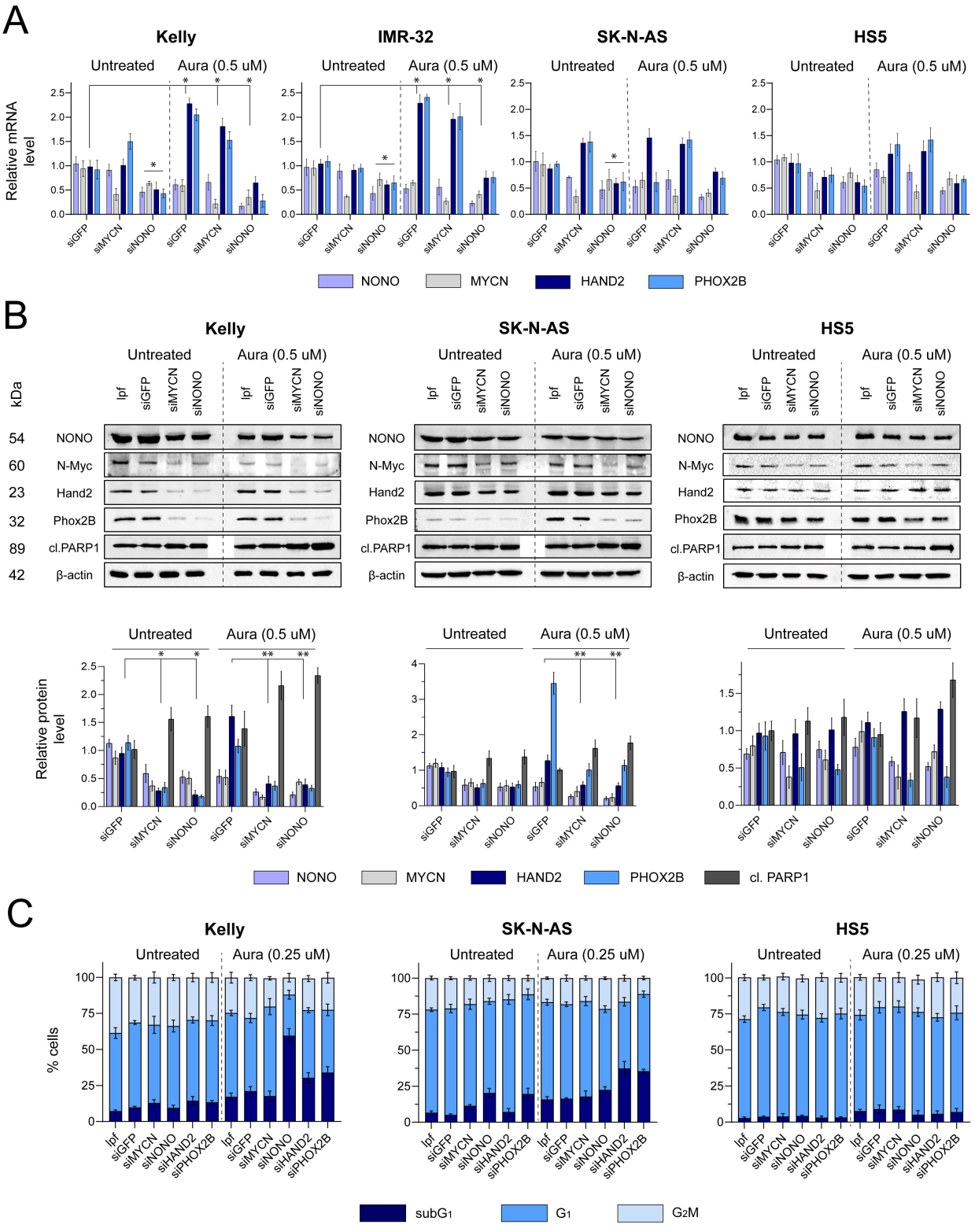

Fig. 2. Auranofin, *NONO* and *MYCN* cooperate for CRC deregulation in NB cell lines. Steady-state levels of CRC mRNAs (A) and proteins (B). (A) Gene-specific signals were normalized to *HPRT1* transcripts. The ratio in untreated cells was taken as 1.0 (control). Bars above the column groups show statistical significance relative to the control. (B) *Top*, immunoblotting of cell lines transfected with siMYCN or siNONO followed by exposure to auranofin. Loading control: β-actin. *Bottom*, densitometric analysis of blots. Levels of protein in mock-transfected (lpf only) cells were taken as 1.0. (C) Cell cycle distribution after treatment with CRC siRNAs ± auranofin. Results are shown as mean values and standard errors (n = 3). $*p \leq 0.05$, $**p \leq 0.01$. See Materials and Methods for details. Aura, auranofin; lpf, liposomes; cl. PARP1- cleaved PARP1 CRC, core regulatory circuitry; NB, Neuroblastoma.

3.3 Auranofin and siNONO Elevate Intracellular ROS

Auranofin induces intracellular ROS accumulation via direct inhibition of the TrxR1 antioxidant enzyme. We addressed the question whether intracellular oxidation evokes death of NB cells with different *MYCN* status. After incubation with siRNAs and auranofin (0.5 µM) cells were stained with YO-PRO™-1 and PI dyes to determine apoptotic *vs.* necrotic components of cell death by flow cytometry. YO-PRO™-1 enters cells with compromised plasma membrane (early apoptosis) and binds to nucleic acids, whereas PI permeates the damaged plasma membrane and intercalates into the DNA (a marker of late-stage apoptosis and/or necrosis). Triton X-100 (0.1%, 5 min) was used as a positive control for PI entry. Fig. 3A and **Supplementary Fig. 3** showed that late apoptotic-necrotic fraction in response to siNONO+auranofin was robust in Kelly and SK-N-AS cell lines (~40%) compared to HS5 fibroblasts (~10%). Accordingly, HS5 cells appear to be less vulnerable to genetic (siRNA) as well as to pharmacological (auranofin) NONO inhibition, suggesting a therapeutic 'window'. Additionally, siNONO alone induced a more pronounced apoptosis in Kelly cells, and synergy of auranofin and siNONO was observed only in this *MYCN*-amplified NB cell line.

Since we observed that auranofin can inactivate NONO on a protein level (Fig. 2B), we hypothesized that this effect stems not as much from direct NONO inhibition by auranofin but from altered intracellular redox balance in response to TrxR1 inhibition. To test this assumption, we examined the effect of auranofin on intracellular ROS generation using flow cytometry-assisted detection of $DCFH_2$-DA dye fluorescence. H_2O_2 (0.5 mM) was used as a control for intracellular ROS accumulation [48]. As shown in Fig. 3B and **Supplementary Fig. 4**, auranofin (0.5 µM) rapidly increased the portion of DCF-bright events in NB cells (Kelly, IMR-32 and SK-N-AS) and, to a lesser extent, in non-malignant HS5 fibroblasts. Importantly, treatment with siNONO phenocopied the ROS-inducing effect of auranofin. Moreover, the combination of 0.5 µM auranofin and siNONO further elevated (up to ~50–75%) the percentage of DCF-bright cells in Kelly and IMR-32 cells.

Next, clonogenic assays were performed to evaluate the long-term effects of siNONO+auranofin combination on NB cell survival. Unlike shorter treatments, these experiments assessed cytotoxic potency via single-cell survival 14 days post-treatment. Fig. 3C shows that, alone, siRNAs *NONO*, *MYCN*, *HAND2* and *PHOX2B* decreased the clonogenic survival whereas the CRC-unrelated siGFP had no effect. Most importantly, each knockdown was synergistic with sublethal (0.25 µM) concentration of auranofin. As in other assays, the most pronounced effect was observed in Kelly cells: siNONO was the most potent alone (~10-fold reduction of colony numbers *vs.* vehicle control) and together with auranofin (~20-fold reduction). In SK-N-AS cells, siRNAs against *HAND2* and *PHOX2B* showed the best inhibitory effects (5–7-fold decrease of colony numbers). In HS5 fibroblasts, the cytotoxicity of auranofin, alone or together with each CRC-specific siRNAs, was significantly lower compared to NB cell lines.

In summary, intracellular ROS generation by submicromolar concentrations of auranofin altered the expression of the *MYCN*, *NONO*, *HAND2* and *PHOX2B* genes in NB cell lines, the *MYCN*-amplified Kelly cell line being the most sensitive. Although each of these genes is differentially regulated by auranofin, the combinations of this drug with knockdown of *NONO* (Kelly) or *HAND2* (SK-N-AS) substantially increased the cytotoxic potency. These data provide evidence in support of CRC members as regulators of redox status in NB cells. This function of NONO has not been previously documented.

4. Discussion

In this study, we identified the multifunctional RNA/DNA-binding protein NONO as a novel regulator of intracellular redox status in NB cells. Transient *NONO* inactivation mimicked ROS generation in response to the TrxR1 antagonist auranofin. Combinations of *NONO* knockdown and auranofin were preferentially cytotoxic for *MYCN*-amplified (ADRN state-related) NB cells. Two lines of evidence support this conclusion: first, auranofin rapidly decreased the abundance of *NONO* mRNA and protein. Second, siNONO phenocopied ROS elevation by auranofin. Intracellular oxidation down-regulated CRC genes *HAND2* and *PHOX2B*. Most importantly, combinations of auranofin and siNONO potently reduced long-term survival of *MYCN*-amplified cells while evoking less pronounced effect in single *MYCN* copy NB cells and sparing non-malignant counterparts. These observations provide evidence for a bidirectional link between NONO and cellular redox homeostasis: oxidation attenuates *NONO* mRNA/protein and, conversely, *NONO* knockdown exacerbates intracellular oxidation.

Mechanistically, several not mutually exclusive models may account for the observed phenomena: (i) direct modification of NONO (e.g., oxidation of redox-sensitive cysteine residues) could impair its binding to nucleic acids or promote proteasomal degradation; (ii) ROS-dependent limitation of availability of NONO-interacting partners (splicing factors, paraspeckle components, or RNA helicases) may reduce NONO stability or function; (iii) NONO loss may derepress transcriptional programs that activate mitochondrial respiration or diminish the antioxidant capacity (for instance, transcriptional down-regulation of glutathione peroxidase 1 in glioblastoma [49]), thereby producing a feed-forward ROS increase. Importantly, our data do not distinguish between these possibilities. The observed decrease in *NONO* mRNA and protein (Fig. 1C, Fig. 2B) could result from transcriptional repression, altered mRNA stability, enhanced proteasomal degradation, or a combination of these events. Disentangling these mech-

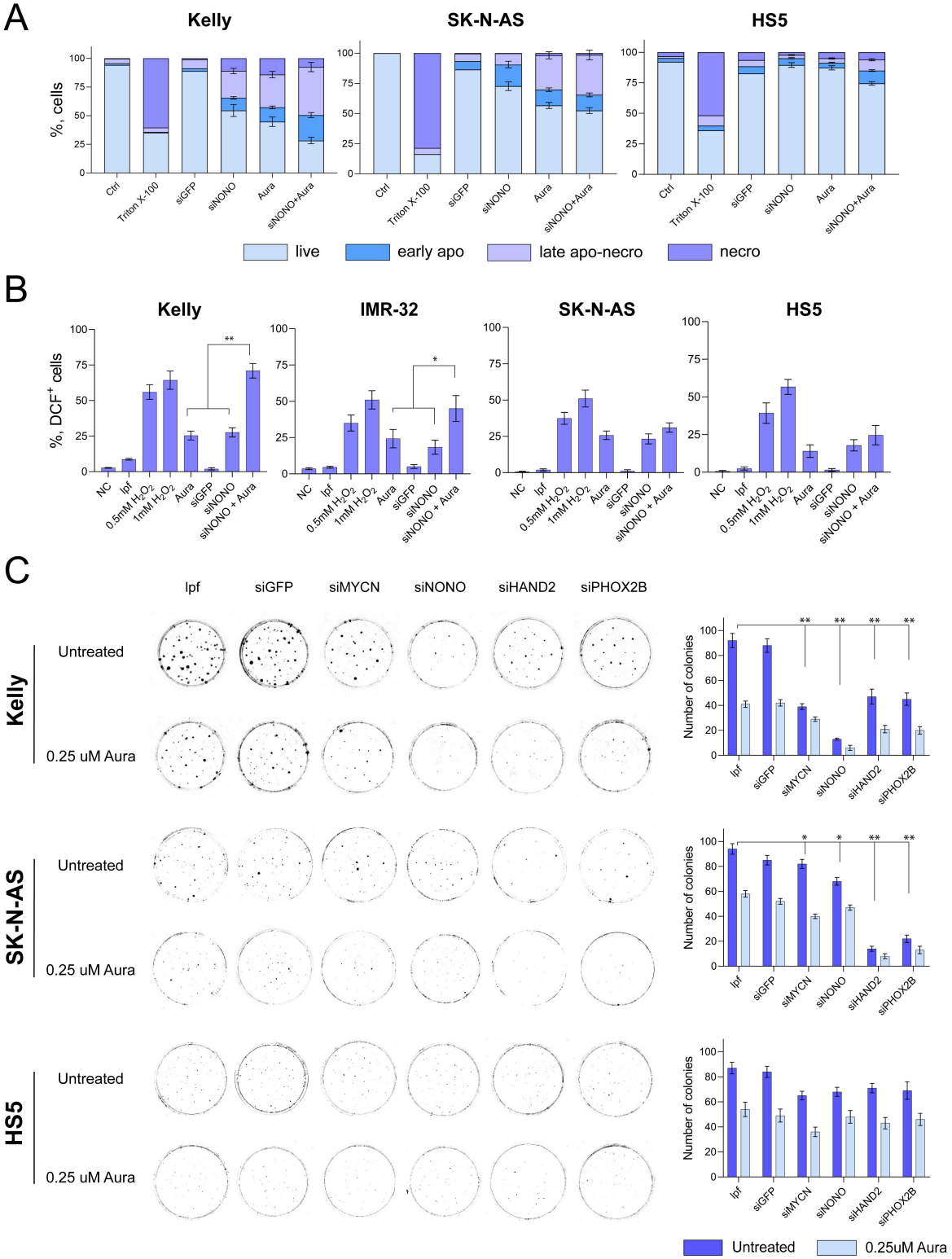

Fig. 3. Effects of auranofin (Aura) and *NONO* knockdown on intracellular ROS content and gene expression. (A) Distribution of cell sub-populations stained with YO-PRO™-1 and PI following gene inactivation (siGFP, siNONO) and auranofin (0.5 µM, 48 h) treatment in Kelly, SK-N-AS and HS5 cell lines. Live, living cells; early apo, early apoptosis; late apo-necro, late apoptosis and necrosis; necro, necrotic fraction. (B) Intracellular ROS generation in cells pre-treated with $DCFH_2$-DA and exposed to indicated agents. Shown are the percentages of cells with elevated ROS (DCF^+). lpf, liposomes. (C) Colony formation assay 14 days after transfection with the respective siRNAs and treatment with 0.25 µM auranofin (24 h). Data are mean ± standard errors (n = 3). *$p \leq 0.05$, **$p \leq 0.01$. See Materials and Methods for details. Aura, auranofin; lfp, liposomes; NC, negative staining control; ROS, reactive oxygen species.

anisms will require measurements of *NONO* mRNA half-life, proteasome inhibition assays, and mass spectrometry-based identification of oxidative post-translational modifications.

It is known that *MYCN* amplification confers a transcriptional and metabolic state characterized by an elevated anabolism and dependence on robust antioxidant systems [50]. Our observation that *MYCN*-amplified cells were preferentially sensitive to auranofin and siNONO is consistent with the hypothesis that CRC integrity and redox status are interdependent vulnerabilities in ADRN NB. This selective vulnerability can be explained by mechanisms inherent in *MYCN* biology. First, *MYCN*-amplified cells operate under constitutive replicative and metabolic stress, leading to a heightened basal ROS load that renders them particularly dependent on antioxidant buffers like Trx system; thus, TrxR1 inhibition by auranofin pushes these cells beyond a critical redox threshold more readily than their non-amplified counterparts [42,50]. Second, the ADRN cell identity maintained by CRC is a hallmark of *MYCN*-amplified tumors, making them exquisitely reliant on the transcriptional coherence. Silencing *NONO* likely causes a disproportionate disassembly of the CRC network, as evidenced by the pronounced downregulation of *HAND2* and *PHOX2B* specifically in the Kelly cell line (Fig. 2A,B). Third, although not directly measured here, elevated NONO expression has been correlated with poor prognosis in NB [34], suggesting that *MYCN*-amplified tumors may exhibit a higher 'oncogenic addiction' to NONO function, making its suppression detrimental. NONO's role in the maintenance of CRC network and association with *MYCN* mRNA [51] surmises that NONO suppression can weaken the transcription-driven proliferation and impair adaptive responses to oxidative stress. The loss of clonogenic survival by the auranofin-siNONO combination likely reflects a collapse of lineage-defining transcription and compensatory antioxidant defenses in cells metabolically stressed by *MYCN* amplification. These findings highlight NONO as an exploitable intersection of transcriptional tuning for adaptation to redox imbalance.

One of the most intriguing findings of this study is the differential regulation of core CRC genes by auranofin and siNONO. While siNONO alone downregulated *HAND2* and *PHOX2B*, auranofin markedly triggered their upregulation, particularly in *MYCN*-amplified cells (Fig. 2A,B). This apparent paradox, i.e., activation of pro-survival genes by a pro-oxidant agent, can be interpreted within a model of a 'compensatory stress response' [42,50]. *MYCN*-driven cells exist in a state of precarious homeostasis, contingent on both robust antioxidant systems and a coherent CRC. We propose that acute oxidative stress induced by auranofin acts as an alarm signal, triggering a rapid transcriptional response to reinforce the core identity by activating its key nodes (*HAND2*, *PHOX2B*). However, when this stress is applied to a cell with compromised CRC network due to NONO inactivation, the compensatory overexpression becomes maladaptive. The cell is forced to execute a transcriptional program without the proper regulatory machinery (NONO) under a prolonged metabolic/redox dysfunction, leading to a collapse. This model explains the dramatic synergy observed in clonogenic assays (Fig. 3C): the initial, seemingly pro-survival signal (auranofin-induced CRC gene expression) creates a state of heightened dependency, making the cell exquisitely vulnerable to NONO suppression. Thus, stress-induced adaptation, when pushed beyond a critical threshold, becomes the trigger for cell death.

Auranofin has a clinical history as an anti-rheumatoid drug owing to its potent and irreversible inhibition of TrxR1 [52]. As a repurposing candidate, auranofin has been explored in cancer treatment. Our data support the concept that transient induction of oxidative stress can lead to targeted destabilization of individual CRC members (HAND2, PHOX2B) to achieve a pronounced long-term lethality in *MYCN*-amplified NB. Importantly, auranofin has been reported to inactivate *NONO* at least indirectly as a part of metabolic response to intracellular oxidation [45]. However, the opportunities of translation of auranofin into clinical oncology, particularly for pediatric tumors, faces considerable challenges. Main limitations include a narrow therapeutic 'window' and dose-limiting adverse systemic effects such as hepatic and renal toxicity [53,54]. Moreover, as a TrxR1 inhibitor, auranofin can affect both tumor and normal cells, which raises concerns about its selectivity. Clinical trials of auranofin monotherapy in solid tumors have shown limited efficacy, likely due to tumor adaptation through compensatory antioxidant pathways [55]. Pharmacokinetics and long-term safety profiles in children remain inadequately studied, necessitating caution [56]. Combinatorial strategies such as pairing low, potentially safer doses of auranofin with targeted molecular interventions like NONO suppression may offer a more viable route to enhance selectivity and reduce off-target toxicity while achieving synergistic anticancer effects [57]. Recent discovery of (R)-SKBG-1 compound that covalently binds to a critical cysteine residue in NONO [35] provided a unique instrument for direct pharmacological NONO inactivation. It is of particular interest to investigate whether (R)-SKBG-1 evokes similar effects on ROS content and CRC gene expression as auranofin and siNONO. Also, protein degraders using (R)-SKBG-1 structure for NONO recognition (PROTAC-like approaches) are likely to be feasible. The fact that auranofin is an approved drug could accelerate early clinical testing of combinations given that safety considerations, particularly systemic oxidative stress and off-target toxicities, are rigorously evaluated. Notably, our data suggest a certain selectivity, as non-malignant HS5 fibroblasts were less susceptible to the combination treatment.

NB displays lineage plasticity between ADRN and MES states, and treatment-induced selection or trans-

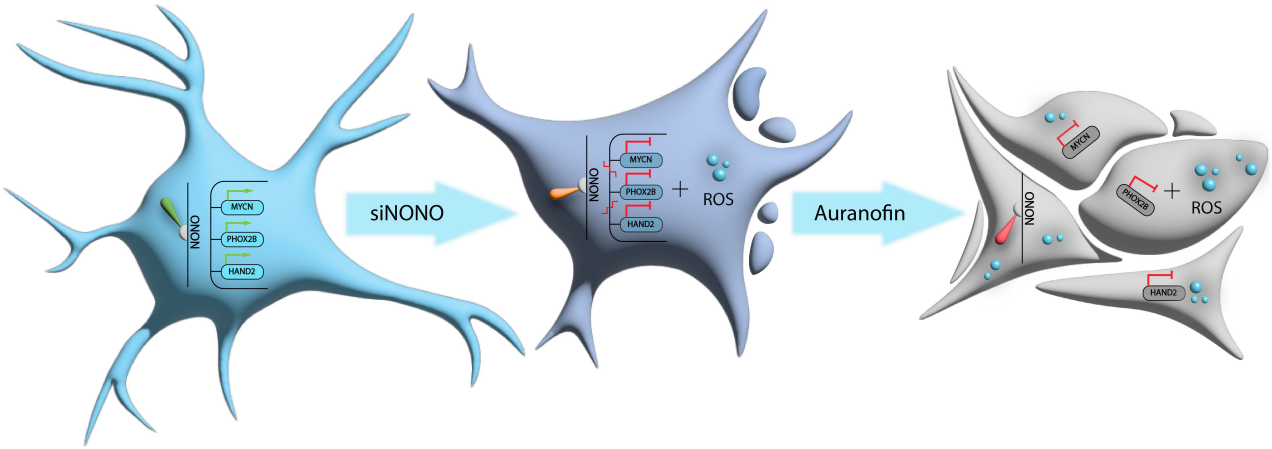

Fig. 4. Auranofin and *NONO* knockdown synergize in triggering intracellular oxidation and death in NB cells. From left to right: intact neurocyte (blue); intracellular ROS generation and altered CRC gene expression in response to auranofin (pink); additional exposure to siNONO exacerbates redox imbalance leading to apoptosis (gray). Blue circles, ROS species; green lines, positive regulation; red lines, down-regulation. Made with Adobe Illustrator 2025.

differentiation toward MES phenotypes has been associated with resistance [15]. Oxidative stress, a condition that accompanies NB growth in a mouse model [58], can favor state transition or select for MES-like cells that survive ROS insult [59]. Alternatively, ROS burst may activate compensatory transcriptional programs that involve *HAND2/PHOX2B* before terminal collapse. Future work should address the question of whether the surviving cells acquire MES phenotype(s) and evaluate the regimens that impede plasticity by combining NONO attenuation with inhibitors of pathways that support MES survival. Likewise, up-regulation of alternative antioxidant systems (glutathione biosynthesis, NADPH-producing enzymes) may produce resistance; profiling adaptive transcriptomic and metabolomic responses will be essential to design durable combinations.

5. Study limitation

We acknowledge that our conclusions regarding NONO's role in maintaining CRC integrity are drawn from changes in expression of *HAND2* and *PHOX2B*, rather than from direct chromatin occupancy or enhancer activity assays. This constitutes a limitation of the current study. However, we argue that these two factors serve as reliable sentinels of CRC functionality in *MYCN*-amplified neuroblastoma for several reasons. First, both *HAND2* and *PHOX2B* are established core components of the ADRN CRC, identified through genome-wide CRISPR screens as essential for the survival of *MYCN*-driven cells [27,28]. Their expression levels are tightly coupled to the functional state of the super-enhancer network that defines this lineage [44]. Second, mechanistic studies have demonstrated that NONO directly binds to and regulates the processing of *HAND2* and other CRC-associated transcripts, acting as a post-transcriptional guardian of this circuitry [31,33]. Therefore, the pronounced downregulation of *HAND2* and *PHOX2B* upon *NONO* knockdown (Fig. 2A,B) is consistent with a disruption of known functions of NONO. While studies employing ChIP-seq for NONO or CRC-associated histone marks (e.g., H3K27ac) are expected to provide a deeper mechanistic insight, our current data establish an initial functional link between NONO suppression, destabilization of key CRC transcription factors, and subsequent cell death.

Moreover, the precise molecular mechanism by which oxidative stress downregulates NONO remains to be further elucidated. While we demonstrated a clear functional link between auranofin-induced ROS, decreased *NONO* expression, and CRC destabilization, our study does not address the question of whether this occurs at the transcriptional, post-transcriptional, or post-translational levels. Although attractive, a possibility that NONO is a direct sensor of redox deregulation requires molecular validation. These open questions highlight the need for transcriptome/proteome analyses and RNA stability assays to map oxidative modifications on NONO and its interacting partners.

6. Conclusion

This study establishes NONO as a mechanistic link between oxidative stress and the core regulatory circuitry in neuroblastoma. We demonstrate a bidirectional relationship in which auranofin-induced ROS downregulate NONO expression, while NONO knockdown itself elevates intracellular ROS. This interplay preferentially destabilizes the adrenergic transcriptional program, leading to suppression of CRC factors HAND2 and PHOX2B and a profound loss of clonogenic survival when NONO attenuation is combined with sublethal oxidative stress (Fig. 4). Importantly, MYCN-amplified cells exhibit heightened sensitivity to this dual insult, whereas non-malignant fibroblasts

remain largely spared. These findings identify NONO as a therapeutically exploitable vulnerability in high-risk neuroblastoma and provide a rationale for combinatorial strategies that disrupt both CRC integrity and redox homeostasis.

Disclosure

The paper is listed as "NONO as a Sensor of Intracellular Oxidation: Relevance to Neuroblastoma Cell Death" as a preprint on bioRxiv at: https://www.biorxiv.org/content/10.1101/2025.10.30.685543v1.

Abbreviations

ADRN, adrenergic; CDKN1A, cyclin-dependent kinase inhibitor 1A; CRC, core regulatory circuitry; GFP, green fluorescent protein; HAND2, heart and neural crest derivatives expressed 2; lpf, liposomes; NB, neuroblastoma; MES, mesenchymal; PHOX2B, paired-like homeobox 2B; ROS, reactive oxygen species; siRNA, small interfering RNA; TrxR1/*TXNRD1*, thioredoxin reductase 1.

Availability of Data and Materials

The raw immunoblotting and flow cytometry data presented in this article are available from the lead contact upon request. The sources of datasets supporting the conclusions of this article are included within the article and its **Supplementary Materials**. All data supporting our findings are available from the corresponding author upon reasonable request.

Author Contributions

Conceptualization: AAS and OAK. Methodology: SSP, OOM, LVM and OAK. Validation: SSP, OOM and LVM. Formal analysis: SSP, OOM and OAK. Data curation: NVA and AAS. Writing original draft: SSP, OOM, LVM, AAS and OAK. Visualization: SSP and OAK. Funding acquisition: NVA. All authors contributed to editorial changes in the manuscript. All authors read and approved the final manuscript. All authors have participated sufficiently in the work and agreed to be accountable for all aspects of the work.

Ethics Approval and Consent to Participate

Not applicable.

Acknowledgment

The authors are grateful to V.S. Leizerovich for providing auranofin, and to Dr. G.S.Kopeina (Moscow State University) for sharing the antibody to cleaved PARP1.

Funding

This work was supported by the Russian Science Foundation, grant 24-15-00097.

Conflict of Interest

The authors declare no conflict of interest.

Supplementary Material

Supplementary material associated with this article can be found, in the online version, at https://doi.org/10.31083/FBL48544.

References

[1] Tomolonis JA, Agarwal S, Shohet JM. Neuroblastoma pathogenesis: deregulation of embryonic neural crest development. Cell and Tissue Research. 2018; 372: 245–262. https://doi.org/10.1007/s00441-017-2747-0.

[2] Lundberg KI, Treis D, Johnsen JI. Neuroblastoma Heterogeneity, Plasticity, and Emerging Therapies. Current Oncology Reports. 2022; 24: 1053–1062. https://doi.org/10.1007/s11912-022-01270-8.

[3] Brodeur GM. Spontaneous regression of neuroblastoma. Cell and Tissue Research. 2018; 372: 277–286. https://doi.org/10.1007/s00441-017-2761-2.

[4] Qiu B, Matthay KK. Advancing therapy for neuroblastoma. Nature Reviews. Clinical Oncology. 2022; 19: 515–533. https://doi.org/10.1038/s41571-022-00643-z.

[5] Lerone M, Ognibene M, Pezzolo A, Martucciello G, Zara F, Morini M, *et al*. Molecular Genetics in Neuroblastoma Prognosis. Children. 2021; 8: 456. https://doi.org/10.3390/children8060456.

[6] Müller M, Trunk K, Fleischhauer D, Büchel G. MYCN in neuroblastoma: The kings' new clothes and drugs. EJC Paediatric Oncology. 2024; 4: 100182. https://doi.org/10.1016/j.ejcped.2024.100182.

[7] Pastorino F, Capasso M, Brignole C, Lasorsa VA, Bensa V, Perri P, *et al*. Therapeutic Targeting of ALK in Neuroblastoma: Experience of Italian Precision Medicine in Pediatric Oncology. Cancers. 2023; 15: 560. https://doi.org/10.3390/cancers15030560.

[8] Carén H, Kryh H, Nethander M, Sjöberg RM, Träger C, Nilsson S, *et al*. High-risk neuroblastoma tumors with 11q-deletion display a poor prognostic, chromosome instability phenotype with later onset. Proceedings of the National Academy of Sciences of the United States of America. 2010; 107: 4323–4328. https://doi.org/10.1073/pnas.0910684107.

[9] Comitani F, Nash JO, Cohen-Gogo S, Chang AI, Wen TT, Maheshwari A, *et al*. Diagnostic classification of childhood cancer using multiscale transcriptomics. Nature Medicine. 2023; 29: 656–666. https://doi.org/10.1038/s41591-023-02221-x.

[10] Sengupta S, Das S, Crespo AC, Cornel AM, Patel AG, Mahadevan NR, *et al*. Mesenchymal and adrenergic cell lineage states in neuroblastoma possess distinct immunogenic phenotypes. Nature Cancer. 2022; 3: 1228–1246. https://doi.org/10.1038/s43018-022-00427-5.

[11] Vayani OR, Kaufman ME, Moore K, Chennakesavalu M, Ter-Haar R, Chaves G, *et al*. Adrenergic and mesenchymal signatures are identifiable in cell-free DNA and correlate with metastatic disease burden in children with neuroblastoma. Pediatr Blood & Cancer. 2024; 71: e30735. https://doi.org/10.1002/pbc.30735.

[12] Wang L, Tan TK, Durbin AD, Zimmerman MW, Abraham BJ, Tan SH, *et al*. ASCL1 is a MYCN- and LMO1-dependent member of the adrenergic neuroblastoma core regulatory circuitry. Nature Communications. 2019; 10: 5622. https://doi.org/10.1038/s41467-019-13515-5.

[13] Shendy NAM, Zimmerman MW, Abraham BJ, Durbin AD. Intrinsic transcriptional heterogeneity in neuroblastoma guides

mechanistic and therapeutic insights. Cell Reports. Medicine. 2022; 3: 100632. https://doi.org/10.1016/j.xcrm.2022.100632.
[14] Boeva V, Louis-Brennetot C, Peltier A, Durand S, Pierre-Eugène C, Raynal V, *et al*. Heterogeneity of neuroblastoma cell identity defined by transcriptional circuitries. Nature Genetics. 2017; 49: 1408–1413. https://doi.org/10.1038/ng.3921.
[15] Naiditch JA, Jie C, Lautz TB, Yu S, Clark S, Voronov D, *et al*. Mesenchymal change and drug resistance in neuroblastoma. The Journal of Surgical Research. 2015; 193: 279–288. https://doi.org/10.1016/j.jss.2014.07.018.
[16] van Groningen T, Akogul N, Westerhout EM, Chan A, Hasselt NE, Zwijnenburg DA, *et al*. A NOTCH feed-forward loop drives reprogramming from adrenergic to mesenchymal state in neuroblastoma. Nature Communications. 2019; 10: 1530. https://doi.org/10.1038/s41467-019-09470-w.
[17] Durbin AD, Versteeg R. Cell state plasticity in neuroblastoma. EJC Paediatric Oncology. 2024; 4: 100184. https://doi.org/10.1016/j.ejcped.2024.100184.
[18] Thirant C, Peltier A, Durand S, Kramdi A, Louis-Brennetot C, Pierre-Eugène C, *et al*. Reversible transitions between noradrenergic and mesenchymal tumor identities define cell plasticity in neuroblastoma. Nature Communications. 2023; 14: 2575. https://doi.org/10.1038/s41467-023-38239-5.
[19] Krystal J, Foster JH. Treatment of High-Risk Neuroblastoma. Children. 2023; 10: 1302. https://doi.org/10.3390/children10081302.
[20] Wawrzuta D, Chojnacka M, Dembowska-Bagińska B, Raciborska A, Hutnik Ł, Cieślak M, *et al*. Revisiting the role of radiotherapy in the treatment of neuroblastoma 4S: 30 years of institutional experience and systematic review. Clinical and Translational Radiation Oncology. 2024; 47: 100791. https://doi.org/10.1016/j.ctro.2024.100791.
[21] Sait S, Modak S. Anti-GD2 immunotherapy for neuroblastoma. Expert Review of Anticancer Therapy. 2017; 17: 889–904. https://doi.org/10.1080/14737140.2017.1364995.
[22] London WB, Castel V, Monclair T, Ambros PF, Pearson ADJ, Cohn SL, *et al*. Clinical and biologic features predictive of survival after relapse of neuroblastoma: a report from the International Neuroblastoma Risk Group project. Journal of Clinical Oncology. 2011; 29: 3286–3292. https://doi.org/10.1200/JCO.2010.34.3392.
[23] Herd F, Basta NO, McNally RJQ, Tweddle DA. A systematic review of re-induction chemotherapy for children with relapsed high-risk neuroblastoma. European Journal of Cancer. 2019; 111: 50–58. https://doi.org/10.1016/j.ejca.2018.12.032.
[24] Fawzy M, Hamoda A, Elhemaly A, Elkinaai N, Soliman S, Reda H, *et al*. Does Salvage Chemotherapy Regimen Intensity Embark on Clearance of Bone Marrow Neuroblastoma? Asian Pacific Journal of Cancer Prevention. 2019; 20: 1519–1524. https://doi.org/10.31557/APJCP.2019.20.5.1519.
[25] Zhou X, Wang X, Li N, Guo Y, Yang X, Lei Y. Therapy resistance in neuroblastoma: Mechanisms and reversal strategies. Frontiers in Pharmacology. 2023; 14: 1114295. https://doi.org/10.3389/fphar.2023.1114295.
[26] Y KN, Arjunan A, Maigandan D, Dharmarajan A, Perumalsamy LR. Advances and challenges in therapeutic resistant biomarkers of neuroblastoma: A comprehensive review. Biochimica et Biophysica Acta. Reviews on Cancer. 2024; 1879: 189222. https://doi.org/10.1016/j.bbcan.2024.189222.
[27] Durbin AD, Zimmerman MW, Dharia NV, Abraham BJ, Iniguez AB, Weichert-Leahey N, *et al*. Selective gene dependencies in MYCN-amplified neuroblastoma include the core transcriptional regulatory circuitry. Nature Genetics. 2018; 50: 1240–1246. https://doi.org/10.1038/s41588-018-0191-z.
[28] Ciaccio R, De Rosa P, Aloisi S, Viggiano M, Cimadom L, Zadran SK, *et al*. Targeting Oncogenic Transcriptional Networks in Neuroblastoma: From N-Myc to Epigenetic Drugs. International Journal of Molecular Sciences. 2021; 22: 12883. https://doi.org/10.3390/ijms222312883.
[29] Gao Y, Volegova M, Nasholm N, Das S, Kwiatkowski N, Abraham BJ, *et al*. Synergistic Anti-Tumor Effect of Combining Selective CDK7 and BRD4 Inhibition in Neuroblastoma. Frontiers in Oncology. 2022; 11: 773186. https://doi.org/10.3389/fonc.2021.773186.
[30] Kuchur OA, Pogodaeva SS, Zhdankina VI, Scherbakova AV, Shtil AA, Antipova NV. Targeting transcription in neuroblastoma: focus on the core regulatory circuit. Expert Opinion on Therapeutic Targets. 2025; 29: 579–595. https://doi.org/10.1080/14728222.2025.2545837.
[31] Pogodaeva SS, Miletina OO, Antipova NV, Shtil AA, Kuchur OA. Saying "Yes" to NONO: A Therapeutic Target for Neuroblastoma and Beyond. Cancers. 2025; 17: 3228. https://doi.org/10.3390/cancers17193228.
[32] Ronchetti D, Traini V, Silvestris I, Fabbiano G, Passamonti F, Bolli N, *et al*. The pleiotropic nature of NONO, a master regulator of essential biological pathways in cancers. Cancer Gene Therapy. 2024; 31: 984–994. https://doi.org/10.1038/s41417-024-00763-x.
[33] Zhang S, Cooper JA, Chong YS, Naveed A, Mayoh C, Jayatilleke N, *et al*. NONO enhances mRNA processing of super-enhancer-associated GATA2 and HAND2 genes in neuroblastoma. EMBO Reports. 2023; 24: e54977. https://doi.org/10.15252/embr.202254977.
[34] Liu PY, Erriquez D, Marshall GM, Tee AE, Polly P, Wong M, *et al*. Effects of a novel long noncoding RNA, lncUSMycN, on N-Myc expression and neuroblastoma progression. Journal of the National Cancer Institute. 2014; 106: dju113. https://doi.org/10.1093/jnci/dju113.
[35] Kathman SG, Koo SJ, Lindsey GL, Her HL, Blue SM, Li H, *et al*. Remodeling oncogenic transcriptomes by small molecules targeting NONO. Nature Chemical Biology. 2023; 19: 825–836. https://doi.org/10.1038/s41589-023-01270-0.
[36] Lindsey GL, Hockley TK, Gomez AV, Marshall AC, Brothers WR, Finney CT, *et al*. Structural and mechanistic analysis of covalent ligands targeting the RNA-binding protein NONO. Cell Chemical Biology. 2026; 33: 256–267.e11. https://doi.org/10.1016/j.chembiol.2025.12.010.
[37] Florio AV, Buré C, Fribourg S. Structural basis for NONO-specific modification by the α-chloroacetamide compound (R)-SKBG-1. Cell Chemical Biology. 2026; 33: 268–275.e3. https://doi.org/10.1016/j.chembiol.2025.12.013.
[38] Abdalbari FH, Telleria CM. The gold complex auranofin: new perspectives for cancer therapy. Discover Oncology. 2021; 12: 42. https://doi.org/10.1007/s12672-021-00439-0.
[39] Chmelyuk N, Kordyukova M, Sorokina M, Sinyavskiy S, Meshcheryakova V, Belousov V, *et al*. Inhibition of Thioredoxin-Reductase by Auranofin as a Pro-Oxidant Anticancer Strategy for Glioblastoma: In Vitro and In Vivo Studies. International Journal of Molecular Sciences. 2025; 26: 2084. https://doi.org/10.3390/ijms26052084.
[40] Mañas A, Seger A, Adamska A, Smyrilli K, Siaw JT, Radke K, *et al*. Targeted ferroptosis induction enhances chemotherapy efficacy in chemoresistant neuroblastoma. NPJ Precision Oncology. 2025; 9: 311. https://doi.org/10.1038/s41698-025-01090-6.
[41] Madeira JM, Bajwa E, Stuart MJ, Hashioka S, Klegeris A. Gold drug auranofin could reduce neuroinflammation by inhibiting microglia cytotoxic secretions and primed respiratory burst. Journal of Neuroimmunology. 2014; 276: 71–79. https://doi.org/10.1016/j.jneuroim.2014.08.615.
[42] Floros KV, Cai J, Jacob S, Kurupi R, Fairchild CK, Shende M, *et al*. *MYCN*-Amplified Neuroblastoma Is Addicted to Iron and Vulnerable to Inhibition of the System Xc-/Glutathione

Axis. Cancer Research. 2021; 81: 1896–1908. https://doi.org/10.1158/0008-5472.CAN-20-1641.

[43] Hou GX, Liu PP, Zhang S, Yang M, Liao J, Yang J, *et al*. Elimination of stem-like cancer cell side-population by auranofin through modulation of ROS and glycolysis. Cell Death & Disease. 2018; 9: 89. https://doi.org/10.1038/s41419-017-0159-4.

[44] Gomez RL, Woods LM, Ramachandran R, Abou Tayoun AN, Philpott A, Ali FR. Super-enhancer associated core regulatory circuits mediate susceptibility to retinoic acid in neuroblastoma cells. Frontiers in Cell and Developmental Biology. 2022; 10: 943924. https://doi.org/10.3389/fcell.2022.943924.

[45] Kim SJ, Ju JS, Kang MH, Eun JW, Kim YH, Raninga PV, *et al*. RNA-binding protein NONO contributes to cancer cell growth and confers drug resistance as a theranostic target in TNBC. Theranostics. 2020; 10: 7974–7992. https://doi.org/10.7150/thno.45037.

[46] Aboelella NS, Brandle C, Kim T, Ding ZC, Zhou G. Oxidative Stress in the Tumor Microenvironment and Its Relevance to Cancer Immunotherapy. Cancers. 2021; 13: 986. https://doi.org/10.3390/cancers13050986.

[47] Cockfield JA, Schafer ZT. Antioxidant Defenses: A Context-Specific Vulnerability of Cancer Cells. Cancers. 2019; 11: 1208. https://doi.org/10.3390/cancers11081208.

[48] Kim H, Xue X. Detection of Total Reactive Oxygen Species in Adherent Cells by 2′,7′-Dichlorodihydrofluorescein Diacetate Staining. Journal of Visualized Experiments. 2020. https://doi.org/10.3791/60682.

[49] Ben Mrid R, El Guendouzi S, Mineo M, El Fatimy R. The emerging roles of aberrant alternative splicing in glioma. Cell Death Discovery. 2025; 11: 50. https://doi.org/10.1038/s41420-025-02323-0.

[50] Veas-Perez de Tudela M, Delgado-Esteban M, Cuende J, Bolaños JP, Almeida A. Human neuroblastoma cells with MYCN amplification are selectively resistant to oxidative stress by transcriptionally up-regulating glutamate cysteine ligase. Journal of Neurochemistry. 2010; 113: 819–825. https://doi.org/10.1111/j.1471-4159.2010.06648.x.

[51] Naveed A. Understanding the Role of RNA-Binding Protein NONO and Its Long Non-Coding RNA Target NEAT1 in Driving Progression of Neuroblastoma [PhD dissertation]. Australia: The University of Western Australia. 2020. https://doi.org/10.26182/5f3f662e6ffdc.

[52] Onodera T, Momose I, Kawada M. Potential Anticancer Activity of Auranofin. Chemical & Pharmaceutical Bulletin. 2019; 67: 186–191. https://doi.org/10.1248/cpb.c18-00767.

[53] Roder C, Thomson MJ. Auranofin: repurposing an old drug for a golden new age. Drugs in R&D. 2015; 15: 13–20. https://doi.org/10.1007/s40268-015-0083-y.

[54] Bonner MY, Vancsik T, Oliveira-Coelho A, Sabatier P, Beusch CM, Zeqiraj K, *et al*. Anti-Tumoral Treatment with Thioredoxin Reductase 1 Inhibitor Auranofin Fosters Regulatory T Cell and B16F10 Expansion in Mice. Antioxidants. 2025; 14: 1351. https://doi.org/10.3390/antiox14111351.

[55] Chen X, Zhou HJ, Huang Q, Lu L, Min W. Novel action and mechanism of auranofin in inhibition of vascular endothelial growth factor receptor-3-dependent lymphangiogenesis. Anticancer Agents in Medicinal Chemistry. 2014; 14: 946–954. https://doi.org/10.2174/1871520614666140610102651.

[56] Spadoni C. Pediatric Drug Development: Challenges and Opportunities. Current Therapeutic Research, Clinical and Experimental. 2019; 90: 119–122. https://doi.org/10.1016/j.curtheres.2018.12.001.

[57] Hua Y, Dai X, Xu Y, Xing G, Liu H, Lu T, *et al*. Drug repositioning: Progress and challenges in drug discovery for various diseases. European Journal of Medicinal Chemistry. 2022; 234: 114239. https://doi.org/10.1016/j.ejmech.2022.114239.

[58] Novotny NM, Grosfeld JL, Turner KE, Rescorla FJ, Pu X, Klaunig JE, *et al*. Oxidative status in neuroblastoma: a source of stress? Journal of Pediatric Surgery. 2008; 43: 330–334. https://doi.org/10.1016/j.jpedsurg.2007.10.040.

[59] Čipak Gašparović A, Milković L, Dandachi N, Stanzer S, Pezdirc I, Vrančić J, *et al*. Chronic Oxidative Stress Promotes Molecular Changes Associated with Epithelial Mesenchymal Transition, NRF2, and Breast Cancer Stem Cell Phenotype. Antioxidants. 2019; 8: 633. https://doi.org/10.3390/antiox8120633.